ADVANCED MATERIALS
www.advmat.de

Efficiency of Polymer Light-Emitting Diodes: A Perspective

*Bas Van der Zee, Yungui Li, Gert-Jan A. H. Wetzelaer, and Paul W. M. Blom**

The various contributions to the external quantum efficiency (EQE) of polymer light-emitting diodes (PLEDs) are discussed. The EQE of an organic light-emitting diode is governed by a number of parameters, such as the electrical efficiency, the photoluminescence quantum yield (PLQY), the optical outcoupling efficiency and the spin statistics for singlet exciton generation. In the last decade, the electrical efficiency has been determined from a numerical PLED device model. More recently, an optical model to simulate the fraction of photons outcoupled to air for PLEDs with a broad recombination zone has been developed. Together with the directly measured PLQY, the EQE of a PLED can then be estimated. However, it has been observed that the measured EQEs of fluorescent PLEDs, including the model system super-yellow poly(*p*-phenylene vinylene) (SY-PPV) often exceed the expected values. To solve this discrepancy, it is demonstrate that the electrical PLED model has to be expanded by the inclusion of triplet–triplet annihilation (TTA), which is shown to be responsible for a substantial EQE enhancement. Experimentally, it is obtained that TTA contributes to a singlet-exciton generation efficiency of ≈40% in SY-PPV PLEDs, giving rise to an EQE of ≈4% instead of the expected value of 2.5%.

1. Introduction

Light-emitting diodes based on organic semiconductors have the potential to be produced on large flexible areas with low cost, low power consumption and color tuning flexibility. Especially conjugated polymers are a suited building block for low-cost printed light-emitting diodes since their solubility can be easily adapted to a printing or coating process. However, a large disadvantage of polymer-based light-emitting diodes (PLEDs) is their relatively low efficiency and lifetime, which has hindered commercialization. The first PLED reported in 1990 was based on poly(*p*-phenylene vinylene) (PPV) with greenish-yellow emission.[1] Since PPV had a poor solubility in organic solvents, it was functionalized with solubilizing side chains to improve solubility.[2] Using alkoxy-based side chains, PPV-derivatives such as poly[2-methoxy-5-(20-ethylhexyloxy)-*p*-phenylene vinylene] (MEH-PPV)[2] and later on the copolymer termed super-yellow PPV (SY-PPV, inset **Figure 1**d)[3] were synthesized. Amongst PPV-based PLEDs the SY-PPV LEDs reached the highest external quantum efficiencies (EQEs) of ≈4% [4,5] and a LT50 lifetime, meaning the time at which the light-output drops to half of its initial value at constant bias, of a few thousand hours at 1000 cd m^{-2}. Although SY-PPV PLEDs were commercialized in small displays of shavers and mobile phones by Philips, their efficiency and lifetime was too low in comparison to multilayer organic LEDs based on evaporated small molecules and the commercial application of PLEDs was discontinued. In spite of the lost industrial interest, MEH-PPV and later SY-PPV have been used as workhorse polymers by the academic community to further understand the electrical and optical characteristics of PLEDs. In the two decades after their discovery, the emphasis was mainly on understanding the charge transport and recombination processes.[6] It was found that the hole transport in PPV diodes is trap free and space-charge limited. The charge-carrier mobility strongly depends on the amount of energetic disorder of hopping sites, which governs the electric-field and charge-carrier-density dependence of the mobility. In contrast to the hole transport, the electron transport is hindered by trapping. The resulting non-radiative recombination of trapped electrons with free holes is a significant loss process in PLEDs, especially at low voltages. For both trap-assisted and emissive bimolecular recombination, the rate coefficients are of the Langevin type, where the limiting step is the diffusion of electrons and holes toward each other under the influence of their mutual Coulombic interaction. The result is that when the electron- and hole mobility and electron trapping parameters are known, the bipolar PLED current and the voltage dependence of the efficiency can be predicted.[6] A typical example is shown in Figure 1 for a 100 nm-thick SY-PPV based PLED. The typical device architectures used for such studies are ITO/PEDOT/SY-PPV/Au for hole-only devices, Al/SY-PPV/Ba/Al for electron-only devices and ITO/PEDOT/SY-PPV/Ba/Al for PLEDs, all on glass substrates. In Figure 1a the current density–voltage (*J*–*V*) characteristics of a SY-PPV hole-only device are plotted as a function of voltage for different temperatures (symbols). The lines are numerical simulations of a drift–diffusion model that includes a field- and density dependent mobility according to the extended Gaussian

B. Van der Zee, Y. Li, G.-J. A. H. Wetzelaer, P. W. M. Blom
Max Planck Institute for Polymer Research
Ackermannweg 10, Mainz 55128, Germany
E-mail: blom@mpip-mainz.mpg.de

The ORCID identification number(s) for the author(s) of this article can be found under https://doi.org/10.1002/adma.202108887.

DOI: 10.1002/adma.202108887

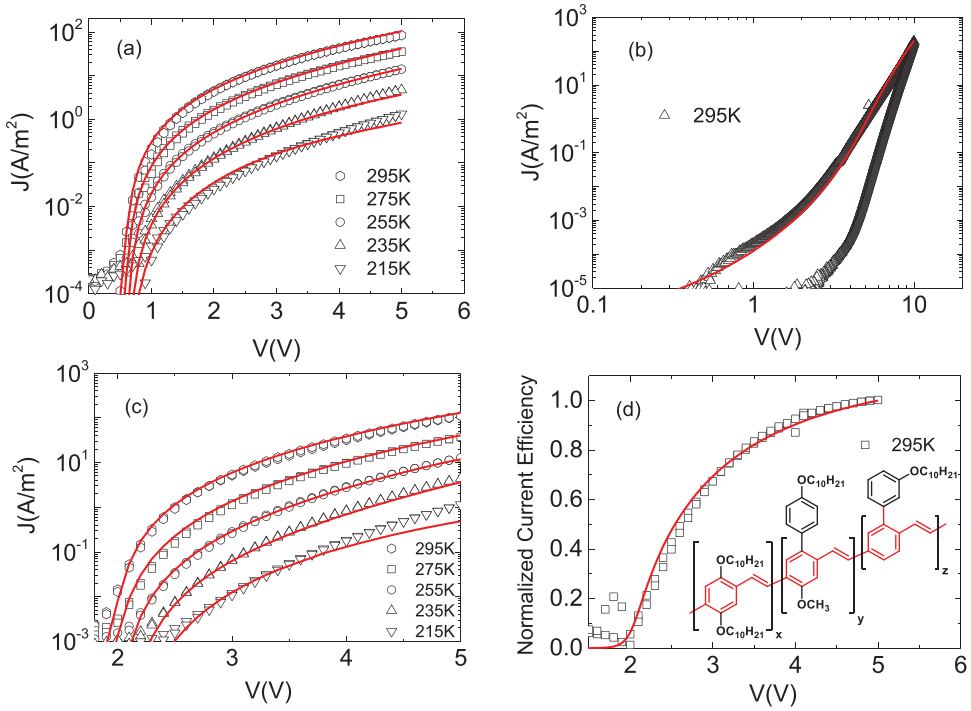

Figure 1. a) Temperature dependent *J–V* characteristics of a hole-only diode of SY-PPV. b) *J–V* characteristic of an electron-only device of SY-PPV, the clockwise hysteresis being due to trapping. c) Temperature-dependent *J–V* characteristics of a double-carrier device (PLED). d) Normalized current efficiency of an SY-PPV PLED at room temperature (I_{ph}/I_{pled}); the inset shows the chemical structure of SY-PPV. All open symbols represent the experimental data for an active layer thickness of L = 100 nm, while the solid lines are numerical simulations. a–d) Reproduced with permission.[9] Copyright 2016, Wiley-VCH.

disorder model (EGDM).[7] The resulting hole mobility at zero field and zero density at room temperature amounts to μ_h (300 K) = 4.8×10^{-12} m^2 V^{-1} s^{-1}. In Figure 1b also the *J–V* of an electron-only device at room temperature is shown (symbols). The model calculations (line) include a Gaussian energy distribution of traps in the bandgap,[8] with parameters the trap density N_t, the trap depth below the LUMO E_t, and the width of the Gaussian trap distribution σ_t. With the trapping parameters $N_t = 1.0 \times 10^{23}$ m^{-3}, E_t = 0.74 eV, and σ_t = 0.1 eV good agreement with experiment is achieved. Using the obtained mobility and trapping parameters the current density and light-output of a SY-PPV PLED are well described, without any free parameters (Figure 1c). Taking into account the quenching of excitons at the metallic cathode[9] also the voltage dependence of the PLED efficiency can be well described. As a result, as reviewed in 2014, the PLED current and light-output were consistently described by a device model incorporating EGDM mobilities, electron trapping and Langevin type of bimolecular and trap-assisted recombination.[6]

One aspect that has received less attention is the absolute value of the PLED efficiency. As shown in Figure 1d, attention was mainly focused on understanding the voltage dependence of the efficiency using normalized values. The external quantum efficiency (EQE) is defined as the ratio between the (observed) emitted photons and injected charge carriers given by[10]

$$\eta_{EQE} = \gamma \cdot \eta_{S/T} \cdot q_{eff} \cdot \eta_{out} \quad (1)$$

where γ is the electrical efficiency, indicating how many excitons are formed relative to the injected amount of charge carriers, $\eta_{S/T}$ the fraction of excitons that decays radiatively due to spin statistics, q_{eff} the photoluminescence quantum yield (PLQY) within the device cavity and η_{out} the fraction of the generated photons able to escape the device to the air mode. For an SY-PPV PLED the electrical efficiency is about 80%, as will be discussed in the next paragraph. Furthermore, for a fluorescent emitter as SY-PPV $\eta_{S/T}$ amounts to 25% and its PLQY is in the range of 60% – 65%.[11] The optical outcoupling is limited by the mismatch of refractive index between the polymer, glass substrate and air that give rise to total internal reflections. Consequently, a large number of generated photons is trapped in the PLED and cannot escape to air. Following classical ray optics, the outcoupling efficiency η_{out} can be approximated by[12]

$$\eta_{out} \approx \frac{1}{2n_{os}^2} \quad (2)$$

with n_{os} the refractive index of the light-emitting polymer. For a typical value of n_{os} = 1.7, only 17% of the generated light is then expected to be collected in the forward hemisphere. Combining all these contributions then would result in an EQE of a SY-PPV PLED in the range of 2.0–2.5%, which is much lower than the reported experimental EQEs of ≈4%.[4,5,11] By carefully analyzing the electroluminescence emission pattern of PPV-based PLEDs, already in 2000 Kim et al. reported that the lower limit for the probability of forming an emissive singlet exciton from electrical injection was not 25%, as expected from spin statistics, but more in the 35%–45% range.[13] However, the origin of the enhanced efficiency was not discussed. In a later study on

triplet dynamics in PLEDs based on poly(9,9′-dioctylfluorene-co-benzothiadiazole) (F8BT), the observed EQE of 6.5%, which largely exceeded the expected EQE of 3.75%, was attributed to triplet–triplet annihilation (TTA), for which a rate constant of $\approx 1 \times 10^{-17}$ m^{-3} s^{-1} was determined.[14] In contrast, from transient electroluminescence measurements on SY-PPV PLEDs it was concluded that the enhanced efficiency above the theoretical maximum is not due to TTA, but arises from an initial singlet/triplet generation ratio larger than 25%.[11] So the origin of the enhanced efficiency in SY-PPV PLEDs and the role of TTA is still controversial. An experimental difficulty is that in fluorescent PLEDs triplet excitons recombine non-radiatively, such that their population and dynamics are hard to track. Herein, the various contributions to the EQE of SY-PPV based PLEDs will be discussed. It is demonstrated that the outcoupling efficiency of a PLED is governed by a combination of a trap-induced position of the recombination zone and the orientation of emitting dipoles. Furthermore, by using an anthracene-based triplet scavenging dye we demonstrate that the efficiency enhancement of SY-PPV PLEDs is the result of TTA, with a rate constant of at least 1×10^{-18} m^{-3} s^{-1}.

2. Electrical Efficiency: Present Status

The availability of a PLED device model allows for a quantification of the various loss processes contributing to the electrical efficiency γ.[15] As an example, in **Figure 2** the calculated contributions from various loss processes to the electrical efficiency of a 120 nm SY-PPV based PLED are shown, as calculated with a drift–diffusion model.

It is observed that at low voltage, non-radiative trap-assisted (Shockley–Read–Hall) recombination is dominant, whereas at higher voltage emissive Langevin recombination takes over due to electron trap-filling, leading to a bias-dependent efficiency. For sufficiently high bias, the Langevin recombination contributes to nearly 80% of the recombination events, implying an electrical efficiency of 0.8. Also indicated in Figure 2 is the estimated contribution of the so-called electrode quenching, which occurs when excitons are formed at a short distance from a metallic electrode due to slow electron transport arising from electron trapping. The energy of these excitons can be transferred to the metallic electrode via long range dipole–dipole interactions, where the exciton energy is dissipated, resulting in efficiency losses. With increasing bias voltage, electron traps are being filled and the recombination zone will move away from the cathode, reducing the relative contribution of the electrode quenching process. In order to estimate the magnitude of these quenching losses a semi-empirical approach has been followed: Using time-resolved photoluminescence on PPV derivatives with varying thickness adjacent to a metallic electrode, it was found that next to the direct energy transfer also diffusion of excitons into the quenching zone contributed to the total efficiency loss. The resulting width of the exciton quenching region of 10–15 nm is governed by the sum of the direct energy transfer length of ≈7.5 nm and the exciton diffusion length L_D of 6 nm. Based on these experiments, a distant dependent exciton quenching profile was used in combination with the recombination profile from the PLED device model.[16] However, it should be noted that these estimated electrode quenching losses, indicated in Figure 2, should not be considered as part of the electrical efficiency when considering the EQE of a PLED. The coupling between photons and electrons in metallic electrodes results in light trapping as surface plasmon polariton (SPP) modes,[17] which are part of the optical outcoupling losses. As a result, to correctly estimate losses due to SPP modes or cathode quenching a full numerical optical model including wavelength dependent refractive indices and emissive dipole orientations should be used. The resulting positional dependence of the outcoupling efficiency then needs to be integrated with the electrical device model, including trapping and trap-assisted recombination. Inclusion of the cathode quenching already in the electrical efficiency would lead to a double counting of these losses. For this reason, the electrical efficiency of a PLED approaches 80% at sufficiently high bias, the 20% losses are the result of trap-assisted recombination.

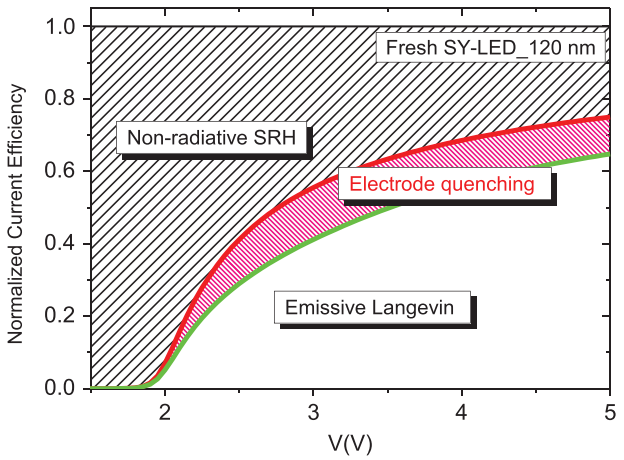

Figure 2. Calculated contributions of the two loss process in a 120 nm SY-PLED. The green lines (solid and dash) show the emissive Langevin recombination. The hashed areas between red and green lines indicate the estimated efficiency loss by electrode quenching. The black dashed areas indicate the efficiency loss due to non-radiative SRH recombination. Reproduced with permission.[9] Copyright 2016, Wiley-VCH.

3. Recent Developments

3.1. Optical Outcoupling for SY-PPV PLEDs

As mentioned above, because of the mismatch of the refractive index of the emissive polymer ($n \approx 1.7$), indium tin oxide ($n \approx 1.8$–2.1), glass substrate ($n \approx 1.5$) and air ($n = 1.0$), not all the generated photons can escape from the device microcavity. The total internal reflections in the various layers result in photon trapping in the organic semiconductor and indium tin oxide (ITO) anode as waveguide modes, in the glass substrate as substrate modes and as SPP modes at the metallic cathode. For multilayer organic LEDs based on evaporated small molecules (OLEDs) with a thin emissive layer, the exciton-generation zone is usually treated as a delta function, i.e., an ultrathin plane in the OLED. Due to this assumption of a fixed recombination zone, the outcoupling efficiency can be estimated by only considering the optical properties of the OLED stack.[18] To enhance

the OLED efficiency, the position of the ultrathin recombination zone is then adjusted to maximize the outcoupling efficiency by tuning the thickness of the charge transport layers.[19,20] However, this approach cannot be followed for the estimation of the optical outcoupling efficiency for single-layer PLEDs for the following reasons: first, the emissive layer of PLEDs can be as thick as hundred nanometers or more, such that the assumption of an ultra-thin emissive plane does not hold. Second, the spatial recombination profile and thus outcoupling efficiency for PLEDs is highly dependent on the charge transport properties (charge carrier mobilities of electrons and holes, trap densities and trap depth) of the active layer, and is therefore also dependent on the driving voltage. Estimation of the optical outcoupling efficiency of a PLED with a broad recombination zone requires a combination of an electromagnetic optical model with electrical numerical drift–diffusion simulations, i.e., integrating knowledge of the local outcoupling efficiency of dipoles with emission from different positions within the broad recombination zone, weighted by the recombination profile from electrical simulations.

3.1.1. Electromagnetic Model

In a PLED, the recombination profile $G(x)$ representing the exciton generation rate per unit volume at different positions x in the active layer is governed by the charge-carrier transport and recombination processes in the organic semiconductor. This profile is obtained from a combination of charge transport studies and numerical drift–diffusion modelling.[6] To calculate the positional dependence of the optical outcoupling efficiency $\eta_{out}(x)$ with the recombination profile $G(x)$ we use the normalized recombination profile $g(x)$, defined as

$$G(x) = \hat{A} \cdot g(x) \tag{3}$$

where $\hat{A}$ is the total exciton concentration generated per unit time per unit area within the entire recombination zone, given by

$$\hat{A} = \int_x G(x)\mathrm{d}x \tag{4}$$

The recombination profile $g(x)$ is then normalized to the integral over the total emissive layer, given by

$$\int_x g(x)\mathrm{d}x = 1 \tag{5}$$

The outcoupling efficiency for a PLED with a broad recombination zone can then be calculated as an integration over η_{out} at different recombination positions, while the weighting function being the sum-normalized recombination profile. The outcoupling efficiency to the air mode is then given by

$$\eta_A = \int_x g(x)\eta_A(x)\,dx \tag{6}$$

The optical outcoupling efficiency to air and substrate modes η_{SA} can be described in a similar way. In this approach the recombination zone is considered as a collection of discrete ultrathin recombination planes, which individually can be described by a delta-function. To obtain the position dependent optical outcoupling efficiencies $\eta_A(x)$ and/or $\eta_{SA}(x)$ the exciton radiative decay and the photon dissipation from the PLEDs are treated as classical electrical dipole antennas, radiating electromagnetic power with a spectrum.[21] The total radiated power $F(\lambda)$, known as the Purcell factor, which has been normalized to the power in free space, is obtained according to:[22]

$$F(\lambda) = \int_0^\infty K(\lambda,u)\,du^2 = 2\int_0^\infty K(\lambda,u)\,du \tag{7}$$

Here, u is the normalized transverse wave vector, defined as $u = k_x/k$, with k_x the parallel wave vector in the plane of the emitting source and k the total wave vector. K is the total spectral power. The orientation factor of the optical transition dipoles (antennas) of these organic emitters can also affect the total radiated power. For an organic emitter with an anisotropic factor a in terms of vertical orientated dipoles, the total spectral power K per unit normalized in-plane wave vector reads:[23]

$$K = aK_{TMv} + (1-a)K_{TMh} + (1-a)K_{TEh} \tag{8}$$

where K_{TMv} is the transverse magnetic (TM) mode from vertically orientated optical dipoles, K_{TMh} the TM mode from horizontally orientated optical dipoles, K_{TEh} the transverse electric (TE) mode from horizontally orientated optical dipoles. The total spectral power $F(\lambda)$ from the organic emitter at a specific wavelength λ then reads:

$$F(\lambda) = 2\int_0^\infty \left[aK_{TMv}(\lambda,u) + (1-a)K_{TMh}(\lambda,u) + (1-a)K_{TEh}(\lambda,u)\right]du \tag{9}$$

The outcoupled power $U(\lambda)$ at wavelength λ to each mode is calculated by integrating the externally radiated power $K_{out}(\lambda,u)$ per unit normalized in-plane wave vector:

$$U(\lambda) = 2\int_0^{u_{crit}(\lambda)} uK_{out}(\lambda,u)\,du \tag{10}$$

The upper integration limit is $u_{crit}(\lambda) = n_o(\lambda)/n_e(\lambda)$, which is the maximum value of the in-plane wave vector for each mode, according to Snell's law. Then, the outcoupling efficiency to each mode for a planar organic light-emitting diode reads:

$$\eta_{out} = \int_\lambda \frac{U(\lambda)}{F(\lambda)}\,d\lambda \tag{11}$$

Therefore, to simulate the outcoupling efficiency at each position inside the emissive layer, one needs to know the device structure and the refractive indices for each layer, the anisotropy factor for the optical transition dipoles and the spectrum in free-space. By integrating the position-dependent outcoupling efficiency over the entire recombination zone, weighted by the sum-normalized recombination profile obtained from electrical device modelling, the optical outcoupling efficiency for a PLED with a broad recombination zone is then obtained.

3.1.2. Recombination Profile

For a single-layer PLED with a neat emissive layer, the position-dependent bimolecular recombination rate can treated as the recombination profile $G(x)$.[6] We note that in the PLED device model[6] processes like singlet-triplet or triplet–triplet

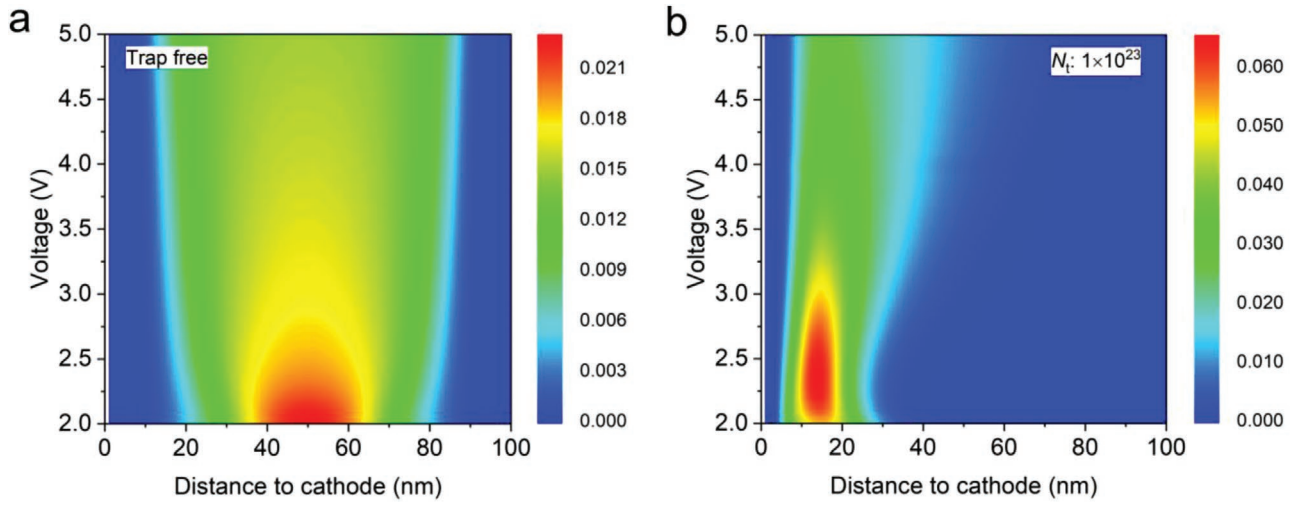

Figure 3. a,b) Voltage and trap density dependent recombination profiles for a 100 nm SY-PPV PLED: a) trap-free; b) electron trap density = 10^{23} m^{-3}. The recombination profile is sum-normalized with a step of 1 nm. a,b) Reproduced with permission.[25] Copyright 2021, The Authors, published by Wiley-VCH.

annihilation are not taken into account yet. The electron trap density N_t in pristine SY-PPV PLEDs typically amounts to a value in the order of 10^{23} m^{-3}, with a Gaussian energy distribution width of about 0.1 eV and a depth of ≈0.7 eV with respect to the LUMO energy.[3]

In **Figure 3**, the recombination profile is shown as a function of the driving voltage for a trap-free PLED (Figure 3a) and for a PLED with an electron trap density N_t of 1×10^{23} m^{-3} (Figure 3b). Since the intrinsic electron and hole mobility of free charge carriers is balanced in PPV-based polymers,[24] the recombination profile within the emissive layer is symmetrical for the trap-free case, as shown in Figure 3a. When adding 10^{23} m^{-3} electron traps, the peak of the recombination profile is close to the cathode at low voltages due to slower electron transport, gradually shifting to the center with increasing driving voltage due to trap filling (Figure 3b). However, for trap densities exceeding 10^{23} m^{-3}, the recombination zone remains close to the cathode, even when the driving voltage is increased to 5 V.[25]

3.1.3. Position Dependent Optical Outcoupling

As described in the electromagnetic model in Section 3.1, the optical constants and the anisotropy factor of the optical dipoles is needed to simulate the position dependent outcoupling efficiency. As shown in **Figure 4**a, the dipole orientation factor for a neat film of SY-PPV is determined by fitting the angular dependence of the *p*-polarized photoluminescence intensity. The orientation of emitting dipoles is represented by the anisotropy factor *a*, which is defined as the fraction of vertical dipoles.[26] Consequently, for fully horizontally (in the plane of the film) oriented dipoles *a* equals zero, for isotropic emitters *a* equals 1/3, and for vertically oriented emitters (perpendicular to the plane of the film) *a* equals 1. From the fit of angular dependence of the *p*-polarized photoluminescence of SY-PPV an anisotropy factor of 0.07 is obtained, indicating that a major fraction of the optical dipoles is horizontally oriented.

According to the electromagnetic modelling (Equations (8), (9)), the positional dependent optical outcoupling efficiency will be higher with a larger proportion of horizontally oriented optical dipoles. As shown in Figure 4b, in case of isotropic emitters (a = 0.333), the maximum optical outcoupling efficiency to air mode $\eta_{A,max}$ is ≈21% at a position with a distance to the cathode of ≈70 nm, while $\eta_{A,max}$ is ≈32% in case of fully horizontal dipoles (a = 0) at a distance to the cathode of ≈60 nm. In the experimental case (a = 0.07), $\eta_{A,max}$ is expected to be around ≈30% at a distance to the cathode of ≈65 nm. For this case, Figure 4b also shows that for emitters in the vicinity of either anode or cathode, the optical outcoupling efficiency is considerably lower as compared to the optimum position in the device cavity. When the emitter is 20 nm away from the metallic cathode, η_A only amounts to ≈10%. **Figure 5**a shows that the outcoupling losses then mainly result from the surface plasmon polariton (SPP) mode. In contrast, when the emissive dipole is 20 nm away from the ITO anode (80 nm from the cathode) η_A is ≈26%, here photons are mainly trapped as substrate and waveguide modes (Figure 5b). With now $\eta_A(x)$ known, as a next step the total optical outcoupling efficiency for a single-layer SY-PPV PLED can be calculated.

3.1.4. Effect of Trap Density on Optical Outcoupling Efficiency

The integrated optical outcoupling efficiency for SY-PPV OLEDs is given by Equation (6), considering the recombination profiles and positional dependent optical outcoupling efficiency. The final position weighted η_A is about 24–26% for a PLED with low trap densities (<1×10^{22} m^{-3}) and the dependence on driving voltages is minor, as shown in **Figure 6**a. The weak voltage dependence is a result of the balanced transport in case of weak trapping, because of which the position of maximum recombination remains in the middle of the device. For PLEDs with a trap density of about 5×10^{22} m^{-3}, the outcoupling efficiency amounts to 14%–22%, depending on the driving voltage. With

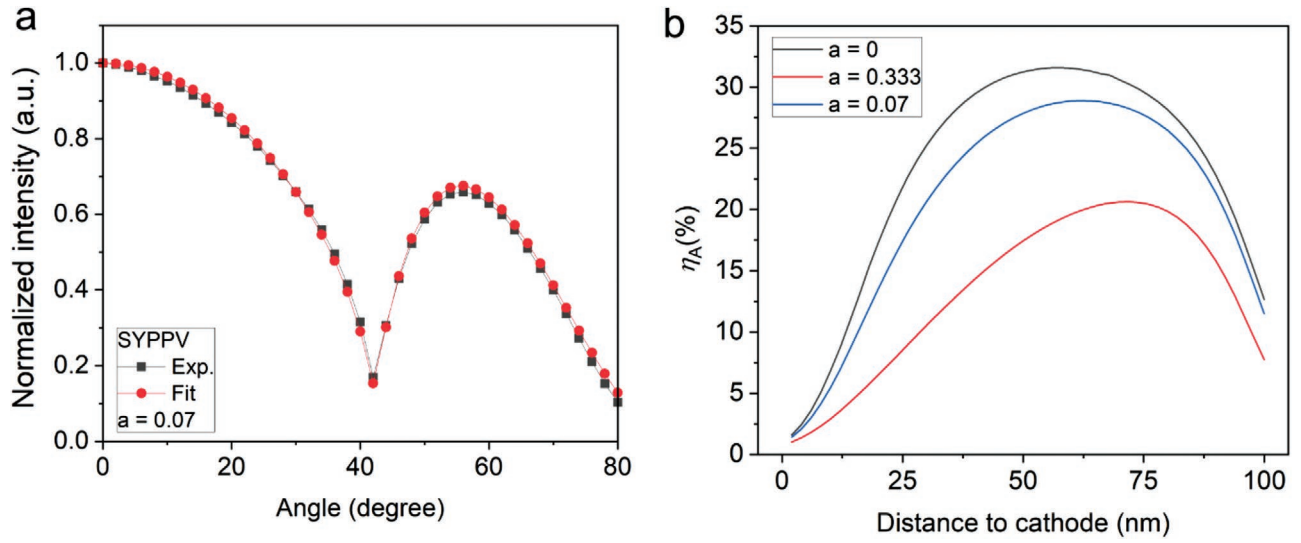

Figure 4. Position-dependent optical outcoupling efficiency for SY-PPV OLEDs. a) Angular dependence of *p*-polarized photoluminescence to determine the anisotropy factor for an SY-PPV neat film in terms of vertical dipoles. b) The position-dependent optical outcoupling efficiency to air mode $\eta_A(x)$ for different anisotropy factors of the dipole moments (isotropic. fully horizontal, experimental value). a,b) Reproduced with permission.[25] Copyright 2021, The Authors, published by Wiley-VCH.

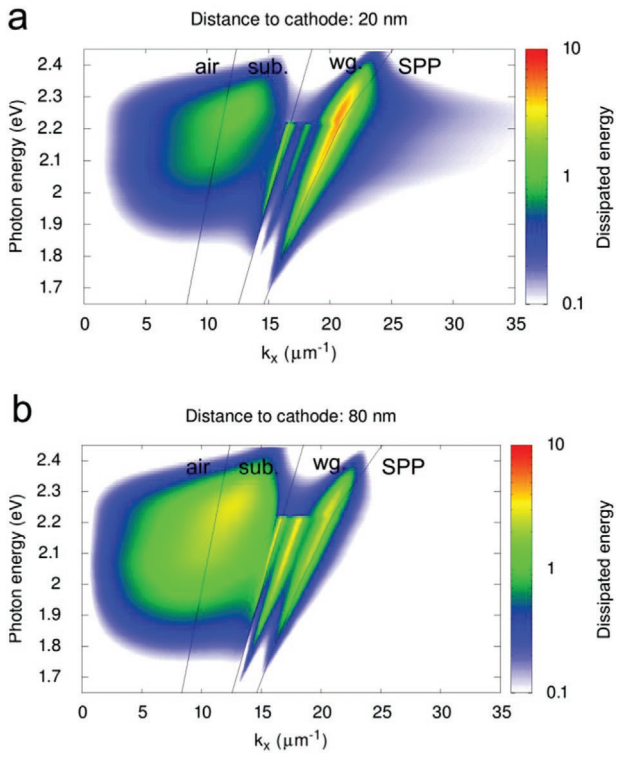

Figure 5. a,b) Energy dissipation for SY-PPV optical dipoles at different positions. The optical simulation is done based on a 100 nm-thick SY-PPV layer with an optical anisotropy factor of 0.07, while the emissive plane is treated as a delta function plane. The emissive plane has a distance to the cathode of 20 nm (a) and 80 nm (b). Air, substrate (sub.), waveguide (wg.) and SPP modes are indicated with respect to the parallel wave vector k_x. a,b) Reproduced with permission.[25] Copyright 2021, The Authors, published by Wiley-VCH.

increasing driving voltage, the recombination zone shifts from the cathode side toward the middle of the PLED (Figure 3b). For $N_t = 1 \times 10^{23}$ m^{-3}, as experimentally observed for SY-PPV, the outcoupling efficiency increases from 10% at 2 V to about 18% at 6.5 V. Finally, the outcoupling efficiency decreases to ≈3% when N_t increases to 1×10^{24} m^{-3}. In this case, due to the large amount of electron traps the recombination stays close to the cathode, even at higher driving voltage, resulting in severe SPP losses. One important conclusion of the obtained results is that outcoupling efficiencies to air of ≈25% are possible in PLEDs when electron trapping is fully suppressed. Second, for a SY-PPV PLED outcoupling efficiencies to air of ≈18% are obtained. This is remarkably close to the estimated value of 17% following classical ray optics (Equation (2)). However, it turns out that this agreement is a coincidence, since the PLED outcoupling is mainly governed by trapping effects via the recombination profile and the nearly fully horizontally oriented emitters of the SY-PPV polymer. To generalize the results to other polymers, in Figure 6b also the effect of the anisotropy factor a on the PLED outcoupling efficiency is shown for a variety of electron trap densities. For a PLED without traps and purely horizontal orientation of dipoles ($a = 0$) a maximum η_A of ≈27% would be possible. We note that variations in electron trap density for different batches of the same polymer might lead to significant variations in the outcoupling efficiency.

3.2. Photoluminescence Quantum Yield

Next to the electrical efficiency γ, governed by charge injection, charge transport and recombination of electrons and holes to form an exciton also the behavior of the excitons prior to their radiative decay is a determining factor for the EQE of a PLED. An exciton, formed either by photo-excitation or Langevin

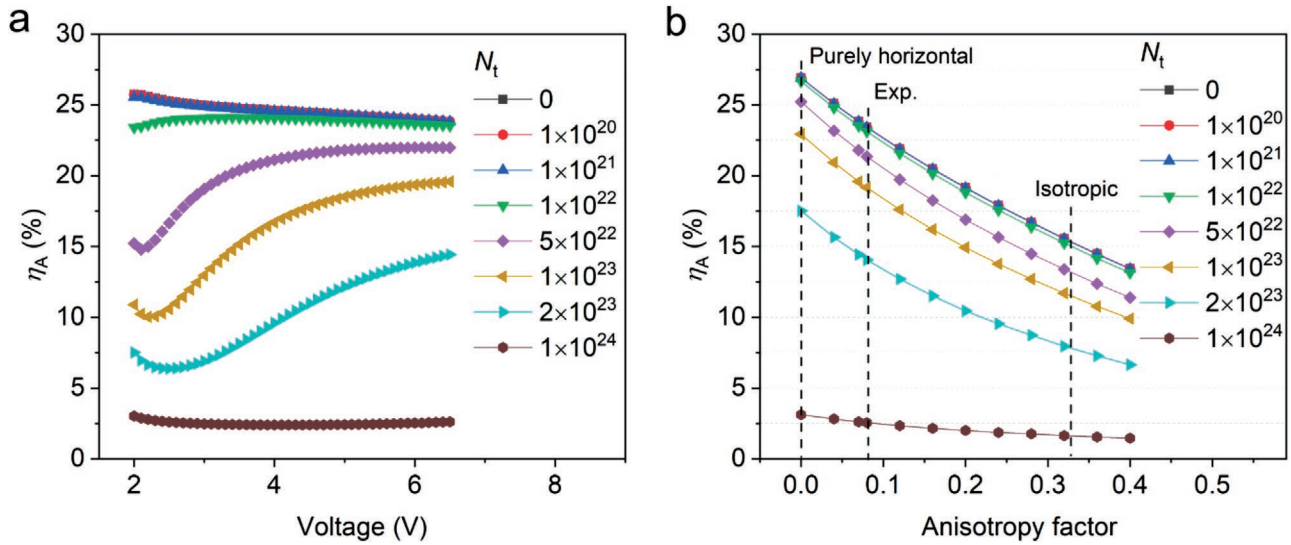

Figure 6. The influence of the trap density on the optical outcoupling efficiency for SY-PPV PLEDs. a) η_A as a function of driving voltage. The used anisotropy factor of 0.07 is experimentally determined for SY-PPV. b) The influence of the anisotropy factor on the outcoupling efficiency η_A for SY-PPV OLEDs at 6.5 V.

recombination in a PLED, will decay back to the ground state within a lifetime τ_f. For devices with a thick emissive layer without strong cavity resonance, the PLQY in free space can be treated as the quantum yield q_{eff} within the device. The photoluminescence lifetime τ_f and the quantum yield q_{eff} are then governed by the intrinsic radiative (k_{rad}) and non-radiative (k_{nonrad}) decay rates, as well as the non-radiative decay related to exciton quenching at defect sites due to exciton diffusion with a rate k_{diff},[27] given by

$$\tau_f = 1/(k_{rad} + k_{nonrad} + k_{diff}) \quad (12)$$

$$q_{eff} = \frac{k_{rad}}{k_{rad} + k_{nonrad} + k_{diff}} \quad (13)$$

It was previously found that τ_f and q_{eff} directly correlate with the energetic disorder of conjugated polymers.[27] Due to increased disorder the diffusion of excitons toward non-radiative quenching sites is slowed down, leading to a strongly enhanced τ_f and q_{eff}. Remarkably, the amount of quenching sites obtained from time-resolved photoluminescence experiments were equal to the amount of electron traps obtained from current-voltage measurements of electron-only devices.[28] This observation strongly suggests that the exciton quenching defects and the electron traps share the same origin. For SY-PPV a q_{eff} in the range of 60–65% has been measured using an integrating sphere. To further enhance q_{eff} it is important to understand where the 35–40% losses originate from. For this purpose, the temperature-dependence of the PL and PLED efficiencies in the PPV derivatives BEH-PPV (poly[2,5-bis(2′-ethyl-hexyl)-1,4-phenylene-vinylene]) and SY-PPV were investigated.[29] The main difference between these two polymers is the different degree of energetic disorder. From charge transport measurements, the width of the Gaussian DOS is determined to be 0.092 eV for BEH-PPV and 0.140 eV for SY-PPV, respectively.[30] It was also observed that in this case the exciton lifetime τ_f. is enhanced by an order of magnitude with increasing disorder, ranging from 180 ps for BEH-PPV to 1.9 ns for SY-PPV.[27] Subsequently, the exciton diffusion coefficient D was obtained from fluorescence quenching experiments using randomly distributed PCBM molecules, known to be efficient exciton quenchers.[27] For SY-PPV it was found that D was temperature activated, ranging from 3.1×10^{-4} cm^2 s^{-1} at room temperature to 8.0×10^{-5} cm^2 s^{-1} at 180 K. In contrast, for the better ordered BEH-PPV, D amounts to 2.5×10^{-3} cm^2 s^{-1}, almost 10 times larger than for SY-PPV. Knowing the PL quantum yield, exciton lifetime, exciton diffusion coefficient and the amount of quenchers/traps, the various contributions to the exciton lifetime and quantum yield q_{eff} can be disentangled: the intrinsic exciton lifetime for both SY-PPV and BEH-PPV amounts to ≈3 ns. For SY-PPV, 25% of the excitons decays non-radiatively and only 10–15% is quenched at a defect site due to the slow exciton diffusion, resulting in an effective exciton lifetime of ≈2 ns and a photoluminescence quantum yield q_{eff} of 60–65%. In contrast, due to reduced disorder and enhanced exciton diffusion in BEH-PPV, almost 90% of the excitons is quenched at a defect site, whereas only 6% decays non-radiatively, resulting in an effective lifetime of only ≈180 ps and a photoluminescence quantum yield q_{eff} of 6%. Since in SY-PPV the diffusion of excitons toward quenchers only plays a minor role at room temperature, a further slowing down of the exciton diffusion by lowering the temperature has only minor effect on q_{eff}, as shown in **Figure 7**a.

The current and light-output of a PLED are both strongly dependent on temperature via the charge carrier mobility. The PLED quantum efficiency, however, defined as the ratio between the light-output as detected photon current and the injected electrical current, is independent on the charge-carrier mobility. Both the current and Langevin recombination rate scale with the mobility, so that it drops out of the efficiency.[31] As a result, the PLED efficiency is expected to be temperature dependent only via q_{eff}. The weak temperature dependence of

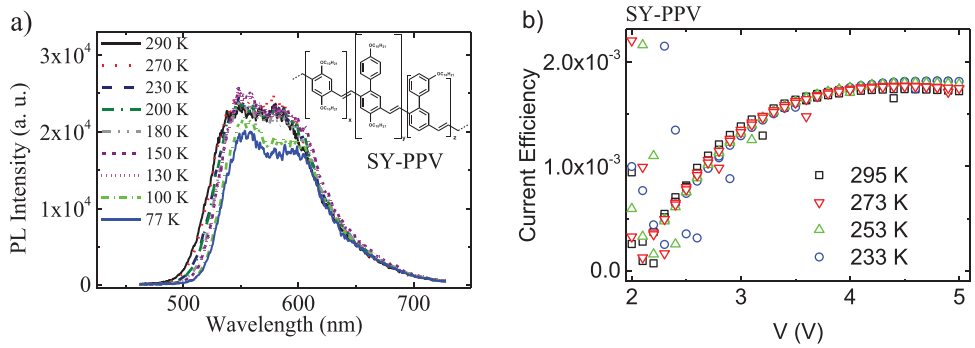

Figure 7. a) Temperature-dependent photoluminescence spectra and b) current efficiency versus voltage of a SY-PPV PLED measured at various temperatures. Reproduced under the terms of the CC-BY Creative Commons Attribution 3.0 Unported license (https://creativecommons.org/licenses/by/3.0).[29] Copyright 2018, RSC Publishing.

q_{eff} for SY-PPV is indeed also reflected in the PLED efficiency, as shown in Figure 7b. In contrast, due to strong contribution of defect quenching to q_{eff} in BEH-PPV, these PLEDs exhibit a strong temperature dependent efficiency; cooling slows down the excitons and the resulting quenching at electron traps, leading to an enhanced efficiency at lower temperatures.[29]

This also explains the trend in early PLED development toward more disordered materials, such as SY-PPV. As shown for BEH-PPV, a decrease in disorder and corresponding increase in the exciton diffusion speed lowers q_{eff} dramatically. However, more disorder also comes at the price of a lower carrier mobility, resulting in a higher operating voltage of the PLED and therefore reduced power efficiency. Due to the steep current-voltage characteristics the increase in voltage going from SY-PPV to BEH-PPV to obtain the same current density is limited to a factor 2–3, which is overwhelmed by the loss of q_{eff}, being an order of magnitude (65% vs 6%, respectively) due to enhanced quenching at defects. As a result, SY-PPV PLEDs are more efficient as compared to their BEH-PPV counterparts. A prerequisite for future PLEDs is therefore the realization of trap-free systems in order to combine high mobility and corresponding fast exciton diffusion with high photoluminescence quantum yield.

4. Next-Generation PLED Device Model

Looking at the various components determining the EQE of a PLED so far, there is yet no obvious reason for the observed EQEs of 4% of SY-PPV PLEDs, instead of the expected 2.5%. The electrical efficiency already amounts to 80%, the outcoupling efficiency is close to 20% and the PLQY of 65% is a directly measured parameter. The only other component is the fraction of excitons that decays radiatively due to spin statistics, $\eta_{S/T}$, which for fluorescent emitters is expected to be 25%.

4.1. Spin Statistics in a SY-PPV PLED

A possible enhancement of this fraction in PLEDs might originate from TTA processes, where non-radiative triplets are converted into radiative singlets.[14] Already in 2003 delayed fluorescence in SY-PPV has been observed that was attributed to the occurrence of TTA.[32] By measuring the conductance and electroluminescence of SY-PPV based PLEDs as function of an external applied magnetic field the occurrence of TTA was identified by a decreases of the electroluminescence with increasing field, reflecting a decreased contribution of TTA to the PLED efficiency.[33] However, in these studies the contribution of the TTA process to the overall PLED efficiency was not determined. What is missing so far for SY-PPV based PLEDs and PLEDs in general is a quantification of the contribution of TTA to the EQE and, if significant, the incorporation of this process in the PLED device model.

The TTA process is represented as:

$$T_1 + T_1 \overset{3/4*k_{TTA}}{\rightarrow} {}^3(TT) \rightarrow S_0 + T_n \rightarrow S_0 + T_1 \tag{14}$$

$$T_1 + T_1 \overset{1/4*k_{TTA}}{\rightarrow} {}^1(TT) \rightarrow S_0 + S_n \rightarrow S_0 + S_1 \tag{15}$$

with ^{3}(TT) as the triplet intermediate and ^{1}(TT) as the singlet intermediate state, $T_1/S_1/S_0$ the triplet/singlet excited, and singlet ground states, respectively, and k_{TTA} the triplet–triplet annihilation rate constant in [m^3 s^{-1}]. It is assumed that the triplet and singlet intermediate state can form with their respective probability of ¾ and ¼. Furthermore, the formation of the quantum mechanically allowed quintet state is omitted, since its energy is too high to be accessible at room temperature.[34]

The contribution of the TTA process to the additional generation of radiative singlet excitons can be described in various ways. Starting with 8 triplets, 6 would annihilate to form 3 triplets (Equation (14)) and 2 triplets would fuse to generate one singlet (Equation (15). Thus, for the generation of 1 singlet exciton, 5 triplet excitons are lost. As a result, the 75% of triplets generated in an OLED would contribute to 0.2 × 75% = 15% of additional singlets, such that the total singlet yield amounts to 25%+15% = 40%.[35] Alternatively, one can argue that for every triplet collision event the fraction f of singlets S_1 formed f amounts to 25%. The triplet states formed by annihilation (Equation (14)) are then recycled as they again can participate in the formation of singlet excitons (Equation (15)). The maximum fraction f_∞ of generated singlets S_1 after recycling then equals to[14]

$$f_\infty = \frac{f}{2}\sum_{n=0}^{n=\infty}\left(\frac{1-f}{2}\right)^n = f\frac{1-f}{1+f} \tag{16}$$

Using $f = 25\%$ then leads to $f\infty = 15\%$, leading again to a total fraction of generated singlet excitons of 40%. It should be noted that this fraction of 40% S_1 generation is a theoretical maximum, since competing loss processes as recombination of triplet excitons are ignored. In order to take direct recombination of triplet excitons into account, we consider the rate equations for singlet and triplet excitons in steady state, which for singlet excitons is given by

$$\frac{d[S(x,t)]}{dt} = \frac{1}{4}\cdot G(x,t) - \frac{[S(x,t)]}{\tau_s} + \frac{1}{4}\cdot k_{\mathrm{TTA}}\cdot[T(x,t)]^2 = 0 \tag{17}$$

$$\frac{[S(x,t)]}{\tau_s} = \frac{1}{4}\cdot G(x,t) + \frac{1}{4}\cdot k_{\mathrm{TTA}}\cdot[T(x,t)]^2 \tag{18}$$

with $[S(x)]$ the singlet density, $G(x)$ the generation rate with x representing the positional dependence and t representing the time dependence, τ_s the singlet lifetime and $[T(x,t)]$ the triplet density. Using the approximation of a uniform generation rate G follows directly from the current density J as:

$$G = \frac{J}{q\cdot d} \tag{19}$$

with d the thickness of the device. The only unknown in Equation (18) is then the triplet density, which can be solved in a similar fashion from the triplet rate equation,

$$\frac{d[T(x,t)]}{dt} = \frac{3}{4}\cdot G(x,t) - \frac{[T(x,t)]}{\tau_t} - \frac{5}{4}\cdot k_{\mathrm{TTA}}\cdot[T(x,t)]^2 = 0 \tag{20}$$

$$[T(x,t)]^2 + \frac{4\cdot[T(x,t)]}{5\cdot k_{\mathrm{TTA}}\cdot\tau_t} - \frac{4\cdot 0.75\cdot G(x)}{5\cdot k_{\mathrm{TTA}}} = 0 \tag{21}$$

with τ_t the triplet lifetime. This quadratic equation has the positive-valued solution

$$[T(x)] = \frac{-2\cdot\tau_t^{-1}}{5\cdot k_{\mathrm{TTA}}} + \sqrt{4\cdot\left(\frac{\tau_t^{-1}}{5\cdot k_{\mathrm{TTA}}}\right)^2 + 4\cdot\frac{0.75\cdot G(x)}{5\cdot k_{\mathrm{TTA}}}} \tag{22}$$

Substitution of Equation (22) into Equation (18) then gives an expression for $[S(x)]/\tau_s$, which is then transformed into the PLED efficiency η according to

$$\eta = \left(\frac{[S(x)]}{\tau_s}\right)/G(x) \tag{23}$$

We note that for $\tau_t \to \infty$ the expression for the triplet concentration (Equation (22)) simplifies to

$$[T(x)] = \sqrt{4\cdot\frac{0.75\cdot G(x)}{5\cdot k_{\mathrm{TTA}}}} \tag{24}$$

which in combination with Equations (18) and (23) also leads to a maximum efficiency 40%.

The rate equation approach also allows us to investigate competition between the two competing process of triplet–triplet annihilation and recombination, characterized by τ_t and k_{TTA}, respectively. For various PPV derivatives a triplet lifetime of ≈100 µs has been obtained,[36–41] whereas for F8BT-based PLEDs a k_{TTA} of $\approx 10^{-17}$ m^{-3} s^{-1} was reported.[14] In **Figure 8** the efficiency for singlet generation is shown as function of the current density where τ_t is fixed at 100 μs and k_{TTA} is varied. As expected, at low current densities the effect of triplet–triplet fusion is limited due to the small triplet concentrations, whereas at higher currents the TTA effect sets in and increases the singlet efficiency from 25% to 40%. For higher k_{TTA} values this process is stronger such that it sets in at lower current densities. Similarly, for a fixed k_{TTA} the enhancement will shift to lower currents for longer triplet lifetimes, since the competing loss process is then weakened. This also means that in a PLED the efficiency enhancement due to TTA will depend on the bias voltage, becoming more important at higher voltages due to the higher triplet concentrations. The exact dependence on voltage will then be governed by the combination of τ_t and k_{TTA}.

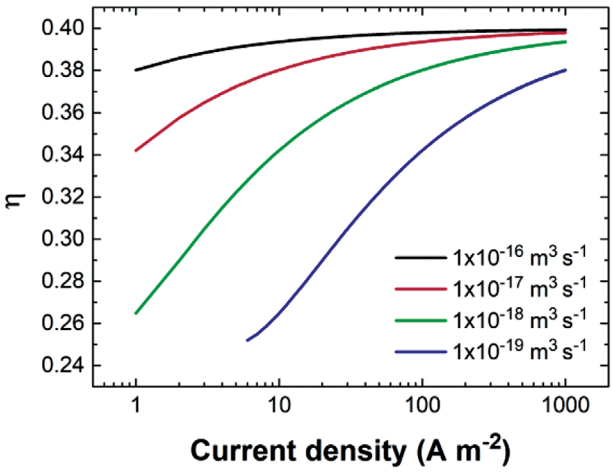

Figure 8. Efficiency of singlet generation as function applied current density for $\tau_t = 100$ μs and varying k_{TTA}.

As discussed in Section 2, in a realistic PLED other loss processes such as trap-assisted recombination also contribute to the efficiency and its voltage dependence. Furthermore, the assumption of a position independent generation rate G is not correct, due to electron trapping most excitons are generated in a region close to the cathode. The additional singlet generation via TTA can be incorporated in the numerical PLED device model by using the local bimolecular Langevin recombination rate $G(x)$. Using Equation (22) then gives the local triplet concentration $T(x)$, which is then substituted in Equation (18) to give the local singlet recombination rate $S(x)/\tau_s$. After integration over the device thickness the total singlet recombination rate per area is then divided by J/q to obtain the PLED efficiency. As an example, in **Figure 9** the numerically calculated product of the electrical efficiency γ and spin-statistics $\eta_{S/T}$ is shown as a function of voltage using the mobility and trapping parameters of SY-PPV, in combination with $k_{\mathrm{TTA}} = 10^{-18}$ m^{-3} s^{-1} and $\tau_t = 100$ µs. As a reference also the trap-free case is shown (dashed lines). For the trap-free case ($\gamma = 100\%$) the maximum efficiency reaches, as expected, 25% without TTA and 40% with TTA, respectively. Furthermore, without TTA there is no voltage dependence due to the absence of a competition between radiative Langevin recombination and non-radiative trap-assisted recombination, whereas the (steep) voltage dependence in the

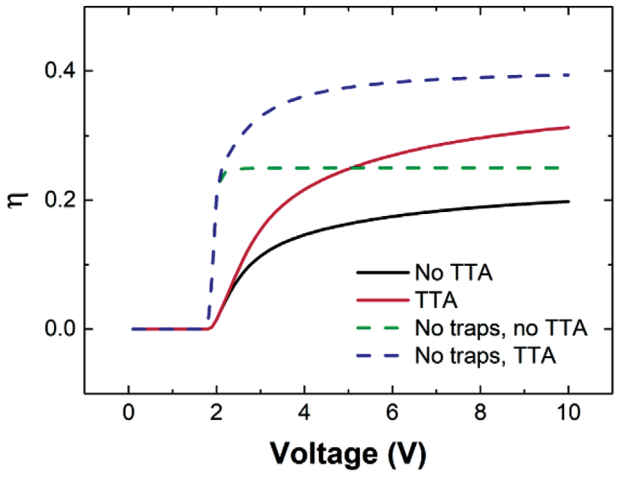

Figure 9. Numerically calculated product $\gamma \times \eta_{S/T}$ as a function of voltage using the mobility and trapping parameters of SY-PPV in the case that $2 \times T_1 > T_N$, in combination with $k_{TTA} = 10^{-18}$ m^{-3} s^{-1} and $\tau_t = 100$ μs (solid lines). Also the trap-free case ($\gamma = 100\%$) is shown (dashed lines).

efficiency reflects the enhanced importance of TTA at higher voltages. In case that electron trapping is included (solid lines) the maximum efficiency is reduced ($\gamma \approx 80\%$) and the voltage dependence is more pronounced due to the abovementioned competition. It should be noted that also in this case TTA enhances the efficiency at 10 V from 20% to 32%, so also a factor of 1.6, similar to the enhancement for the trap-free case (25% vs 40%). This results shows that the relative contribution of TTA to the PLED efficiency is not dependent on the presence of electron traps.

A special case occurs when the triplet intermediate has an energy higher than S_1, but below T_2. Then, triplet annihilation (Equation (14)) is not possible, the intermediate will dissociate again into $2T_1$. Since the formation of excited singlet excitons is still energetically allowed (Equation (15)), half of the triplet excitons can be converted into singlet excitons, leading to a maximum theoretical quantum efficiency of 25%+½ × 75% = 62.5%. This situation is found for example in rubrene or particular anthracene derivatives.[42,43] Also this case can be represented by rate equations, given by

$$\frac{d[S(x,t)]}{dt} = \frac{1}{4}\cdot G(x,t) - \frac{[S(x,t)]}{\tau_s} + k_{TTAUPC}\cdot[T(x,t)]^2 = 0 \quad (25)$$

$$\frac{[S(x,t)]}{\tau_s} = \frac{1}{4}\cdot G(x,t) + k_{TTAUPC}\cdot[T(x,t)]^2 \quad (26)$$

$$\frac{d[T(x,t)]}{dt} = \frac{3}{4}\cdot G(x,t) - \frac{[T(x,t)]}{\tau_t} - 2\cdot k_{TTAUPC}\cdot[T(x,t)]^2 = 0 \quad (27)$$

$$[T(x,t)]^2 + \frac{[T(x,t)]}{2\cdot k_{TTAUPC}\cdot\tau_t} - \frac{0.75\cdot G(x)}{2\cdot k_{TTAUPC}} = 0 \quad (28)$$

$$[T(x)] = \frac{-\tau_t^{-1}}{2\cdot k_{TTAUPC}} + \sqrt{\frac{1}{16}\left(\frac{\tau_t^{-1}}{k_{TTAUPC}}\right)^2 + \frac{0.75\cdot G(x)}{2\cdot k_{TTAUPC}}} \quad (29)$$

where k_{TTAUPC} represents the annihilation coefficient between two triplets in case only upconversion is considered. If every triplet is upconverted ($\tau_t \to \infty$), the expression for the triplet density becomes:

$$[T(x)] = \sqrt{\frac{0.75\cdot G(x)}{2\cdot k_{TTAUPC}}} \quad (30)$$

from which it follows that, as expected, the maximum efficiency is given by

$$\eta_{max} = 0.25 + 0.375 = 0.625 \quad (31)$$

Also this specific case can be incorporated in the PLED device model by inserting the local triplet concentration (Equation (29)) into Equation (26), from which after integration over the device thickness and dividing by J/q the PLED efficiency is obtained. In **Figure 10** the numerically calculated efficiency is shown for a PLED with thickness 110 nm as function of k_{TTA}. Similar to the case where also excited triplet formation is included (Figure 9) the inclusion of trapping (γ = 80%) reduces the maximum efficiency to about 50%. Furthermore, the maximum efficiency of 50% is reached for k_{TTA} larger than 10^{-18} m^{-3} s^{-1}, whereas a maximum close to 40% is obtained for k_{TTA} in the range of 10^{-20} m^{-3} s^{-1}.

Experimentally, delayed fluorescence in SY-PPV due to TTA had been observed using a palladium tetraphenyltetrabenzoporphyrin triplet sensitizer.[44] Here, triplets are photoexcited in the sensitizer and subsequently transferred to SY-PPV, leading to delayed fluorescence after TTA. In SY-PPV PLEDs, however, the contribution of TTA to the overall efficiency has not yet been quantified, hindered by the fact that triplets are not emissive. For this purpose, we blend SY-PPV with the anthracene derivative 9,10-bis(phenylethynyl)anthracene (BPEA) (**Figure 11**a).[45] BPEA is chosen for its high singlet-triplet splitting as compared to SY-PPV. As schematically indicated in Figure 11b due to this high splitting the T_1 level of BPEA (1.11 eV)[44] is lower in energy than the T_1 level of SY-PPV (1.3 eV),[46] such that triplets generated in a SY-PPV:BPEA blend PLED are efficiently transferred from SY-PPV to BPEA. To capture most of the triplet excitons generated in SY-PPV during PLED operation we add BPEA in a concentration

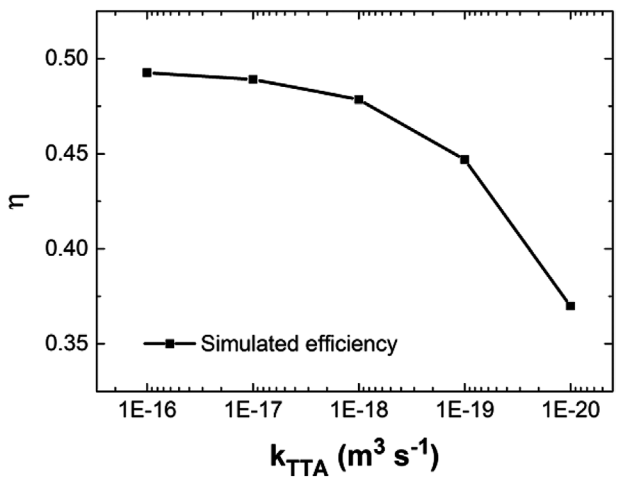

Figure 10. Numerically calculated product $\gamma \times \eta_{S/T}$ at a fixed voltage (8 V) as function of the triplet–triplet annihilation rate k_{TTA} using the mobility and trapping parameters of SY-PPV and $\tau_t = 100$ μs in case that $2 \times T_1 < T_N$.

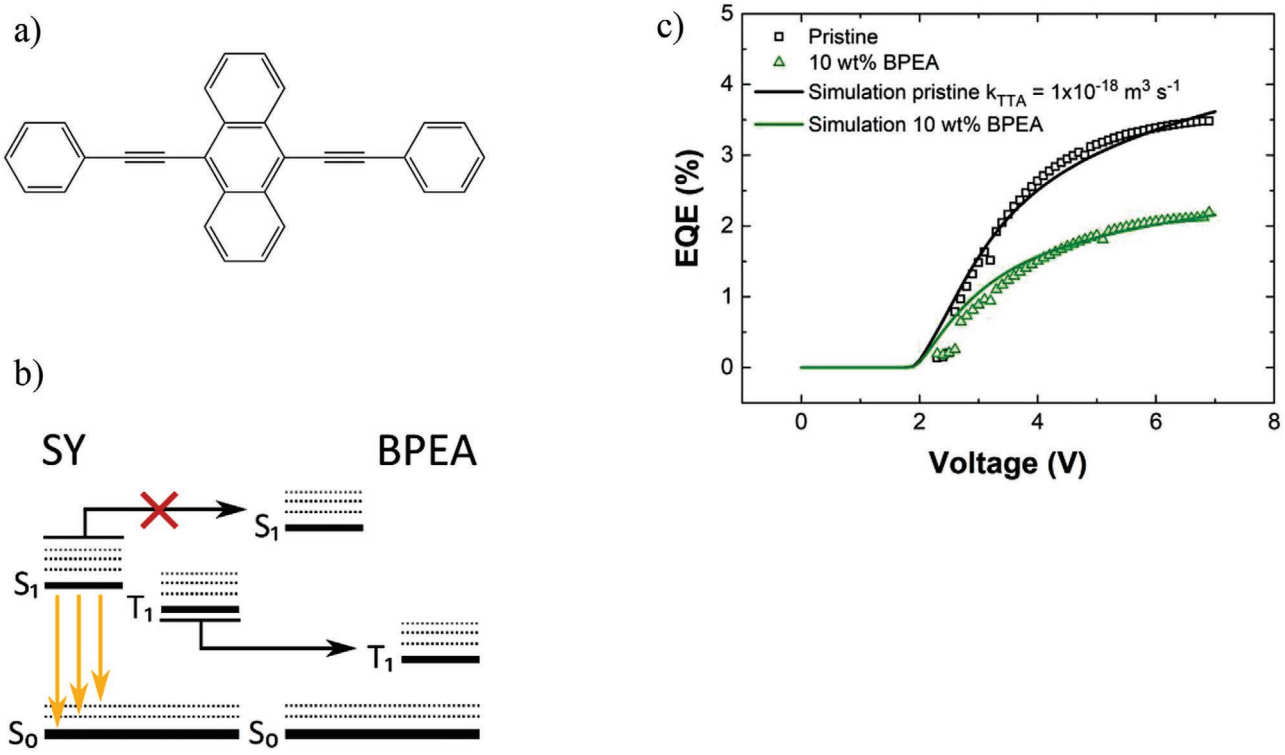

Figure 11. a) Chemical structure of BPEA. b) Schematic energy diagram of the SY-PPV:BPEA system. c) EQE of a SY-PPV PLED with and without 10 wt% of BPEA as a function of voltage (symbols). The solid lines are numerical calculations. a,b) Reproduced with permission.[45] Copyright 2020, The Authors, published by Wiley-VCH.

of 10 wt%. In this way TTA in SY-PPV:BPEA PLEDs is suppressed, which, if TTA is an important process, should also affect the efficiency of the PLED. It should be noted that the singlet level of SY-PPV (2.21 eV)[44] lies below that of the BPEA (2.4 eV),[44] excluding Förster energy transfer of singlet excitons from SY-PPV to BPEA, evidenced by the fact that addition of BPEA does not affect the EL spectra of the SY-PPV PLED.[45] Furthermore, since the HOMO level of BPEA (–5.49 eV)[47] is slightly deeper than the HOMO of SY-PPV (≈–5.4 eV) and the LUMO of BPEA (–2.92 eV)[47] is marginally shallower than the LUMO of SY (≈–2.8 eV) BPEA does not lead to additional charge trapping This is an important point since additional trapping would modify the recombination profile and therefore the outcoupling efficiency and as a result also the EQE. We verified that the *J-V* characteristics of the PLEDs are indeed not affected by the addition of BPEA. In Figure 11c the efficiency of a SY-PPV without and with 10 wt% BPEA is shown as a function of voltage. It is observed that addition of BPEA lowers the EQE of the SY-PPV PLED from 3.5% to 2.2%. First, the EQE of the SY-PPV:BPEA blend PLED is in the range of the expected EQE of 2.0–2.5% without TTA, as discussed in Section 1. Furthermore, the EQE enhancement by a factor of 1.6 without BPEA is exactly what would be expected when TTA increases the spin-statistics for singlet formation from 25% to 40% (Figure 8). The solid lines in Figure 11c represent the numerically modelled EQE versus voltage curves. The EQE of the pristine SY-PPV can be modelled using a k_{TTA} of at least 10^{-18} m^{-3} s^{-1}, which agrees with the earlier reported value for F8BT based PLEDs.[14] As shown in Figure 10, a further increase of k_{TTA} has only minor effect on the efficiency. A question that remains is whether triplets formed by triplet–triplet annihilation (Equation (20)) play a role in SY-PPV or not. It was argued from absorption measurements that for SY-PPV the T_1–T_N gap amounts to 1.5 eV whereas T_1 equals 1.3 eV, meaning that $2 \times T_1 < T_N$.[44] In this case, triplet generation by triplet–triplet annihilation (Equation (20)) would not play a role, such that singlets could be generated with a maximum efficiency of 62.5%. Applying Equations (25)-(29) with more efficient singlet generation to the pristine SY-PPV PLED device model reduces the required k_{TTA} to 10^{-20} m^{-3} s^{-1} to explain the enhanced efficiency. It should be noted that in the SY-PPV:BPEA blend PLED TTA could also potentially play a role. Triplets transferred to BPEA might upconvert to the singlet S_1 state of BPEA, which then could be transferred to the S_1 state of SY-PPV. However, this recombination pathway is expected to be unimportant, since the efficiency of the upconversion reaction via TTA was reported to be only 1.6% for BPEA.[48]

In summary, the observed efficiency enhancement of a factor of 1.6 by inclusion of TTA in the SY-PPV PLED fits very well with the TTA model where both excited singlets and triplet are formed (Equations (17)–(22)), increasing the spin-statistics for singlet generation from 25% to 40%. However, from the efficiency alone the model with 50% efficiency for upconversion of triplets to singlets (Equations (25)–(29)) cannot be excluded, although the strongly reduced k_{TTA} to explain the observed EQE enhancement in that case seems less realistic when compared with values for other polymeric systems obtained from transient experiments.[14]

5. Outlook

A main conclusion from the work presented here is that the presence of electron traps has a triple negative effect on the EQE of a PLED. First, it lowers the electrical efficiency by non-radiative trap-assisted recombination. Second, it lowers the optical outcoupling efficiency by pinning the recombination zone close to the cathode, and third, it lowers the photoluminescence quantum yield due to excitons that diffuse toward traps and are quenched after their formation. For future efficient PLEDs it is therefore essential to realize a trap-free system. It has recently been found that an energy window exists inside which organic semiconductors show trap-free charge transport. Typically, electron trapping occurs in materials with an electron affinity lower than 3.6 eV, whereas hole trapping occurs for organic semiconductors with an ionization energy higher than 6 eV.[49] However, since the ionization energy of most light-emitting polymers such as PPVs was designed to be around ≈5 eV to match the work function of anodes like indium-tin-oxide and poly((3,4-ethylenedioxythiophene) polystyrene sulfonate) (PEDOT:PSS) to obtain efficient hole injection, the PLED efficiency so far is mainly hindered by electron trapping associated with the low electron affinity of typical light-emitting polymers. Furthermore, although TTA is helpful in raising the EQE of PLEDs, it is not an option to achieve PLEDs with a 100% internal quantum efficiency.

Here, a promising route is the development of polymers with a reduced singlet-triplet energy gap that can transfer non-radiative triplet excitons to emissive singlet excitons using the thermal energy from the ambient environment, resulting in thermally activated delayed fluorescence (TADF).[50] A major step toward a trap-free single layer organic LED employing TADF has recently been made, using the small-molecular compound 9,10-bis(4-(9H-carbazol-9-yl)-2,6-dimethylphenyl)-9,10-diboraanthracene (CzDBA) as yellow TADF emitter. This emitter has is HOMO and LUMO energy located within the trap-free energy window, leading to nearly trap-free transport for electrons and holes. In a simplified device architecture with a neat film of CzDBA (75 nm), sandwiched between two Ohmic contacts, a maximum external quantum efficiency (η_{EQE}) of ≈19% has been obtained.[51] In this device, internal quantum efficiencies exceeded 90%.[52] Furthermore, due to the absence of blocking layers causing barriers at the heterojunctions, very low operating voltages were achieved, resulting in a high power efficiency of 90 lm W^{-1}. The strong power efficiency enhancement as compared to the early SY-PPV PLEDs of 15 lm W^{-1} is the combined result of elimination of charge trapping and triplet-exciton harvesting. This result shows that, conceptually, solution-processed organic and polymeric LEDs combining a simple device architecture and high efficiency are possible. We note that for OLEDs exploiting phosphorescence or TADF the TTA process does not enhance the EQE, but is a loss process. Ideally, in these OLEDs every triplet exciton is converted into an emissive species, leading to a 100% internal quantum efficiency. However, in case of TTA two triplets lead to only one singlet instead of two, such that the maximum internal quantum efficiency will be below 100%. This reduced efficiency by TTA is typically observed as an efficiency roll-off at high current densities.[53]

A challenge still to overcome is that the trap-free energy window of 2.5 eV is smaller than the 3 eV bandgap of blue-emitting PLEDs. A way toward trap-free blue emitting PLEDs is the concept of trap-dilution, where trapping effects are strongly reduced by blending the polymer with an insulator, in case phase separation can be prevented.[54]

Acknowledgements

B.V.d.Z. and Y.L. contributed equally to this work.
Open access funding enabled and organized by Projekt DEAL.

Conflict of Interest

The authors declare no conflict of interest.

Keywords

device physics, external quantum efficiency, outcouping efficiency, polymer light-emitting diodes

Received: November 3, 2021
Published online:

[1] J. H. Burroughes, D. D. C. Bradley, A. R. Brown, R. N. Marks, K. Mackay, R. H. Friend, P. L. Burns, A. B. Holmes, *Nature* **1990**, *347*, 539.
[2] D. Braun, A. J. Heeger, *Appl. Phys. Lett.* **1991**, *58*, 1982.
[3] H. Spreitzer, H. Becker, E. Kluge, W. Kreuder, H. Schenk, R. Demandt, H. F. M. Schoo, *Adv. Mater.* **1998**, *10*, 1340.
[4] S. Burns, J. MacLeod, T. T. Do, P. Sonar, S. D. Yambem, *Sci. Rep.* **2017**, *7*, 40805.
[5] Y. Li, O. Sachnik, B. van der Zee, K. Thakur, C. Ramanan, G. A. H. Wetzelaer, P. W. M. Blom, *Adv. Opt. Mater.* **2021**, 9, 2101149.
[6] M. Kuik, G. A. H. Wetzelaer, H. T. Nicolai, N. I. Crăciun, D. M. De Leeuw, P. W. M. Blom, *Adv. Mater.* **2014**, *26*, 512.
[7] W. F. Pasveer, J. Cottaar, C. Tanase, R. Coehoorn, P. A. Bobbert, P. W. M. Blom, D. M. de Leeuw, M. A. J. Michels, *Phys. Rev. Lett.* **2005**, *94*, 206601.
[8] H. T. Nicolai, M. M. Mandoc, P. W. M. Blom, *Phys. Rev. B* **2011**, *83*, 195204.
[9] Q. Niu, G.-J. A. H. Wetzelaer, P. W. M. Blom, N. I. Crăciun, *Adv. Electron. Mater.* **2016**, *2*, 1600103.
[10] T. Tsutsui, E. Aminaka, C. P. Lin, D. U. Kim, *Philos. Trans. R. Soc. London* **1997**, 355, 801.
[11] P. Wang, Q. Huang, S. Zhao, Z. Qin, Z. Xu, D. Song, B. Qiao, *Org. Electron.* **2019**, *68*, 45.
[12] B. E. A. Saleh, M. C. Teich, *Fundamentals of Photonics*, John Wiley & Sons, Inc., New York **2019**.
[13] J. S. Kim, P. K. H. Ho, N. C. Greenham, R. H. Friend, *J. Appl. Phys.* **2000**, *88*, 1073.
[14] B. H. Walikewitz, D. Kabra, S. Gelinas, R. H. Friend, *Phys. Rev. B.* **2012**, *85*, 045209.
[15] M. Kuik, L. J. A. Koster, A. Dijkstra, G. A. H. Wetzelaer, P. W. M. Blom, *Org. Electron.* **2012**, *13*, 969.
[16] D. E. Markov, P. W. M. Blom, *Appl. Phys. Lett.* **2005**, *87*, 233511.
[17] W. L. Barnes, A. Dereux, T. W. Ebbesen, *Nature* **2003**, *424*, 824.
[18] M. Furno, R. Meerheim, S. Hofmann, B. Lüssem, K. Leo, *Phys. Rev. B* **2012**, *85*, 115205.
[19] S. Hofmann, M. Thomschke, P. Freitag, M. Furno, B. Lüssem, K. Leo, *Appl. Phys. Lett.* **2010**, *97*, 2008.
[20] R. Meerheim, M. Furno, S. Hofmann, B. Lüssem, K. Leo, *Appl. Phys. Lett.* **2010**, *97*, 253305.
[21] K. A. Neyts, *J. Opt. Soc. Am. A* **1998**, *15*, 962.
[22] E. M. Purcell, *Phys. Rev.* **1946**, *69*, 37.

[23] M. J. Jurow, C. Mayr, T. D. Schmidt, T. Lampe, P. I. Djurovich, W. Brütting, M. E. Thompson, *Nat. Mater.* **2016**, *15*, 85.
[24] Y. Zhang, B. de Boer, P. W. M. Blom, *Phys. Rev. B* **2010**, *81*, 085201.
[25] Y. Li, B. Van der Zee, G. A. H. Wetzelaer, P. W. M. Blom, *Adv. Electron. Mater.* **2021**, *7*, 2100155.
[26] W. Brütting, J. Frischeisen, T. D. Schmidt, B. J. Scholz, C. Mayr, *Phys. Status Solidi A* **2013**, *210*, 44.
[27] I. Rörich, O. V. Mikhnenko, D. Gehrig, P. W. M. Blom, N. I. Craˇciun, *J. Phys. Chem. B* **2017**, *121*, 1405.
[28] O. V. Mikhnenko, M. Kuik, J. Lin, N. van der Kaap, T.-Q. Nguyen, P. W. M. Blom, *Adv. Mater.* **2014**, *26*, 1912.
[29] I. Rörich, A.-K. Schönbein, D. K. Mangalore, A. Halda Ribeiro, C. Kasparek, C. Bauer, N. I. Craˇciun, P. W. M. Blom, C. Ramanan, *J. Mater. Chem. C* **2018**, *6*, 10569.
[30] D. E. Markov, C. Tanase, P. W. M. Blom, J. Wildeman, *Phys. Rev. B* **2005**, *72*, 045217.
[31] P. W. M. Blom, M. J. M. De Jong, S. Breedijk, *Appl. Phys. Lett.* **1997**, *71*, 930.
[32] S. Sinha, A. P. Monkman, *Appl. Phys. Lett.* **2003**, *82*, 4651.
[33] N. Chitraningrum, T.-Y. Chua, P.-T. Huang, T.-C. Wen, T.-F. Guo, *Org. Electron.* **2018**, *62*, 505.
[34] A. Köhler, H. Bässler, *Mater. Sci. Eng.* **2009**, *R66*, 71.
[35] D. Y. Kondakov, T. D. Pawlik, T. K. Hatwar, J. P. Spindler, *J. Appl. Phys.* **2009**, *106*, 124510.
[36] L. C. Lin, H. F. Meng, J. T. Shy, S. F. Horng, L. S. Yu, C. H. Chen, H. H. Liaw, C. C. Huang, K. Y. Peng, S. A. Chen, *Phys. Rev. Lett.* **2003**, *90*, 036601.
[37] J. Partee, E. L. Frankevich, B. Uhlhorn, J. Shinar, Y. Ding, T. J. Barton, *Phys. Rev. Lett.* **1999**, *82*, 3673.
[38] C. Vijila, M. Westerling, H. Aarniob, R. Österbacka, H. Chun, C. Zhikuan, Z. Xinhai, Z. Furong, C. Soo Jin, *J. Photochem. Photobiol. A* **2008**, *199*, 358.
[39] K. Pichler, D. A. Halliday, D. D. C. Bradley, R. H. Friend, P. L. Burn, A. B. Holmes, *Synth. Metals* **1993**, *55–57*, 230.
[40] A. P. Monkman, H. D. Burrows, L. J. Hartwell, L. E. Horsburgh, I. Hamblett, S. Navaratnam, *Phys. Rev. Lett.* **2001**, *86*, 1358.
[41] M. Scharber, *Ph.D thesis*, University of Linz, Linz, Austria **2002**, https://www.jku.at/fileadmin/gruppen/166/Publikationen/Thesis/Scharber-Diss.pdf
[42] C.-J. Chiang, A. Kimyonok, M. K. Etherington, G. C. Griffiths, V. Jankus, F. Turksoy, A. P. Monkman, *Adv. Funct. Mater.* **2013**, *23*, 739.
[43] D. Di, L. Yang, J. M. Richter, L. Meraldi, R. M. Altamimi, A. Y. Alyamani, D. Credgington, K. P. Musselman, J. L. MacManus-Driscoll, R. H. Friend, *Adv. Mater.* **2017**, *29*, 1605987.
[44] V. Jankus, E. W. Snedden, D. W. Bright, V. L. Whittle, J. A. G. Williams, A. P. Monkman, *Adv. Funct. Mater.* **2013**, *23*, 384.
[45] B. van der Zee, Y. Li, G.-J. A. H. Wetzelaer, P. W. M. Blom, *Adv. Opt. Mater.* **2021**, 9, 2100249.
[46] Y. J. Bae, G. Kang, C. D. Malliakas, J. N. Nelson, J. Zhou, R. M. Young, Y. L. Wu, R. P. Van Duyne, G. C. Schatz, M. R. Wasielewsk, *J. Am. Chem. Soc.* **2018**, *140*, 15140.
[47] C. Wang, Y. Liu, Z. Ji, E. Wang, R. Li, H. Jiang, Q. Tang, H. Li, W. Hu, *Chem. Mater.* **2009**, *21*, 2840.
[48] V. Gray, A. Dreos, P. Erhart, B. Albinsson, K. Moth-Poulsen, M. Abrahamsson, *Phys. Chem. Chem. Phys.* **2017**, *19*, 10931.
[49] N. B. Kotadiya, A. Mondal, P. W. M. Blom, D. Andrienko, G. J. A. H. Wetzelaer, *Nat. Mater.* **2019**, *18*, 1182.
[50] H. Uoyama, K. Goushi, K. Shizu, H. Nomura, C. Adachi, *Nature* **2012**, *492*, 234.
[51] N. B. Kotadiya, P. W. M. Blom, G.-J. A. H. Wetzelaer, *Nat. Photonics* **2019**, *13*, 765.
[52] Y. Li, N. B. Kotadiya, B. van der Zee, P. W. M. Blom, G. A. H. Wetzelaer, *Adv. Opt. Mater.* **2021**, *9*, 2001812.
[53] B. van der Zee, Y. Li, G. A. H. Wetzelaer, P. W. M. Blom, *Adv. Opt. Mater.* **2021**, *9*, 2001812.
[54] D. Abbaszadeh, A. Kunz, G.-J. A. H. Wetzelaer, J. J. Michels, N. I. Crăciun, K. Koynov, I. Lieberwirth, P. W. M. Blo, *Nat. Mater.* **2016**, *15*, 628.

Bas van der Zee received his B.S. and M.S. degree in physics from the University of Groningen, Netherlands. Currently he is a Ph.D. candidate in the group of Prof. Dr. P.W.M. Blom at the MPI for Polymer Research in Mainz, where his research focuses on charge transport and degradation of organic light-emitting diodes.

Yungui Li obtained his B.Sc. and M.Sc. at Huazhong University of Science and Technology. He completed his Ph.D. on photon generation and dissipation in organic light–emitting diodes (OLEDs) at TU Dresden in 2019. He then joined the Molecular Electronics department of the Max Planck Institute for Polymer Research (MPIP) as a postdoc, working on optical outcoupling efficiency for OLEDs. In 2021, he started to work as a group leader in MPIP. His research interest lies in the field of photophysics of organic semiconductors and optoelectronic devices.

Gert-Jan A. H. Wetzelaer obtained his M.Sc. degree in applied physics at the University of Groningen in 2009. In 2014, he obtained a Ph.D. degree with highest honors from the University of Groningen. His doctoral research focused on charge transport and recombination in organic light-emitting diodes and solar cells. Subsequently, he continued as a postdoctoral researcher investigating biophotovoltaic cells involving photosynthetic proteins. In 2015, he obtained a position as group leader at the Max Planck Institute for Polymer Research in Mainz, Germany. His research focuses on device physics of organic light-emitting diodes and solar cells, as well as perovskite solar cells.

Paul W. M. Blom received his Ph.D. degree in 1992 from the Technical University Eindhoven on picosecond charge carrier dynamics in GaAs. At Philips Research Laboratories, he was engaged in the electro-optical properties of polymer light-emitting diodes. From 2000 he held a professorship at the University of Groningen in the field of electrical and optical properties of organic semiconducting devices. In September 2008 he became Scientific Director of the Holst Centre in Eindhoven, where the focus is on foil-based electronics, followed in 2012 by an appointment as director at the MPI for Polymer Research in the field of molecular electronics.